Zhang et al. Journal of the European Optical Society-Rapid Publications (2021) 17:7
https://doi.org/10.1186/s41476-021-00152-z

Journal of the European Optical Society-Rapid Publications

SHORT REPORT Open Access

Raman spectroscopic detection of interleukin-10 and angiotensin converting enzyme

Shuo Zhang*, Frederieke A. M. van der Mee, Roel J. Erckens, Carroll A. B. Webers and Tos T. J. M. Berendschot

Abstract

In this report we present a confocal Raman system to identify the unique spectral features of two proteins, Interleukin-10 and Angiotensin Converting Enzyme. Characteristic Raman spectra were successfully acquired and identified for the first time to our knowledge, showing the potential of Raman spectroscopy as a non-invasive investigation tool for biomedical applications.

Keywords: Confocal Raman spectroscopy, Interleukin-10, Interleukin-21, Angiotensin converting enzyme

Introduction

Recently, a proof-of-concept for molecular profiling of Interleukin-10 (IL-10), Interleukin-21 (IL-21) and Angiotensin Converting Enzyme (ACE) was reported by Kuiper et al. to classify four important ocular conditions affecting the retina [1]. IL-10 plays a crucial role in preventing inflammatory and autoimmune pathologies of several diseases [2]. IL-21 not only has key roles in antitumor and antiviral responses but also has major effects on inflammatory responses [3]. ACE plays an important role among other things in the immune system and regulation of blood flow. It can be elevated in granulomatous diseases [4]. Acquiring information about these molecules in ocular system could help in a better understanding of the complex underlying pathophysiology. Kuiper et al. used a multiplex immunoassay based on Luminex technology to measure the proteins. In this flow cytometry based method a fluorescent signature can be detected on bead-based assays. However, to reach the pg/mL detection limit, sample preparation is complicated and time consuming [5]. Other techniques for cytokines detection and quantification can reach such concentrations, like surface enhanced Raman spectroscopy (SERS) [6–10], high performance liquid chromatography (HPLC) [11], pyro-concentrator (PC) [12, 13], mass spectrometry (MS) [14] etc.. Although the sensitivity of these techniques is comparable or higher than methods using immunoassays, they all need a biopsy to acquire the sample invasively and test in vitro. In HPLC and MS the biomolecule from the sample needs to be fed into the instrument and measured via a chemical or physical process. SER requires matrix assist for signal enhancement which limited its non-destructive applications. Similarly, PC accumulates the target biomolecules from a drop of sample on a chip resulting from the electro-hydrodynamic effect [7, 12]. In addition, electrochemical based biosensors with the combination of optoelectronic components could realize the chip-based biological monitoring by refractive index change [15, 16]. These techniques meet the detection limit requirements of the biomolecules with low volume sample size, which might be challenging for an in vivo measurement, especially testing the chemical composition inside an intact aqueous environment like aqueous humor. In a clinical setting, a preferred option would be a non-invasive and non-destructive technique [17]. We propose to use Raman spectroscopy as a non-invasive and non-destructive sampling technique [8, 17–21]. In this study, IL-10, IL-21 and ACE samples were tested. The characteristic Raman spectra of IL-10 and ACE are

* Correspondence: s.zhang@maastrichtuniversity.nl
University Eye Clinic Maastricht, Maastricht, The Netherlands

presented for the first time, which may pave the way for the development of a non-invasive molecular evidence-based investigation tool in future.

Methods

The basic configuration of the confocal Raman system used in this study was described in a prior article [19]. In short: a 671 nm, 21 mW continuous wave diode laser (Ignis 671, Laser Quantum) was used as an excitation source for the wavenumber region between 2500 and 4000 cm^{-1} and a 785 nm, 23 mW continuous wave diode laser (SM 785 nm, Innovative Photonic Solutions) was used as an excitation source for wavenumber range between 350 cm^{-1} and 1800 cm^{-1}. The two lasers were both connected via single-mode optical fibers to a Raman module (HPRM 2500, River Diagnostics®) and spectra were recorded in both regions individually. In the current configuration. The microscope objective lens used in the prior work was replaced by an achromatic lens (focal length = 80 mm, Linos). It acts both to focus the laser on the sample and to collect the Raman scattered light. A charge-coupled device camera (operating temperature: − 65°), integrated within the spectrometer acquired the spectra with a spectral resolution of 2 cm^{-1} in both wavenumber regions. Samples of IL-10 were supplied by BD Bioscience (BD 554611), IL-21 by ThermoFisher Scientific (Catalog # 14–8219-62) and ACE by R&D systems (Catalog # 929-ZN-010). The samples were transported on dry ice and, when arrived, immediately stored at − 80°. All samples were solved in filtrated (0.22 um filter) 0.1% bovine serum albumin (BSA) in phosphate buffered saline (PBS). The IL-10 sample contained 10 μl with a concentration of 5.0 ng/ml. The IL-21 and ACE sample each had a total volume of 10 μl with a concentration of 10.0 ng/ml. All samples were tested in fused silica cuvettes after they were moved from the − 80° freezer and thawed to room temperature.

Spectra of IL-10 and ACE samples were acquired with 60s integration times. For IL-21 the integration time was 300 s. For all samples, two sequential spectra with same integration time were obtained at the same focus area to determine the characteristic Raman peaks and rule out disturbances of cosmic rays. The signal-to-noise ratio (SNR) for each sample was calculated by dividing the intensity of the highest signal peak by the sample standard deviation of the spectral region of 1750 cm^{-1} to 1800

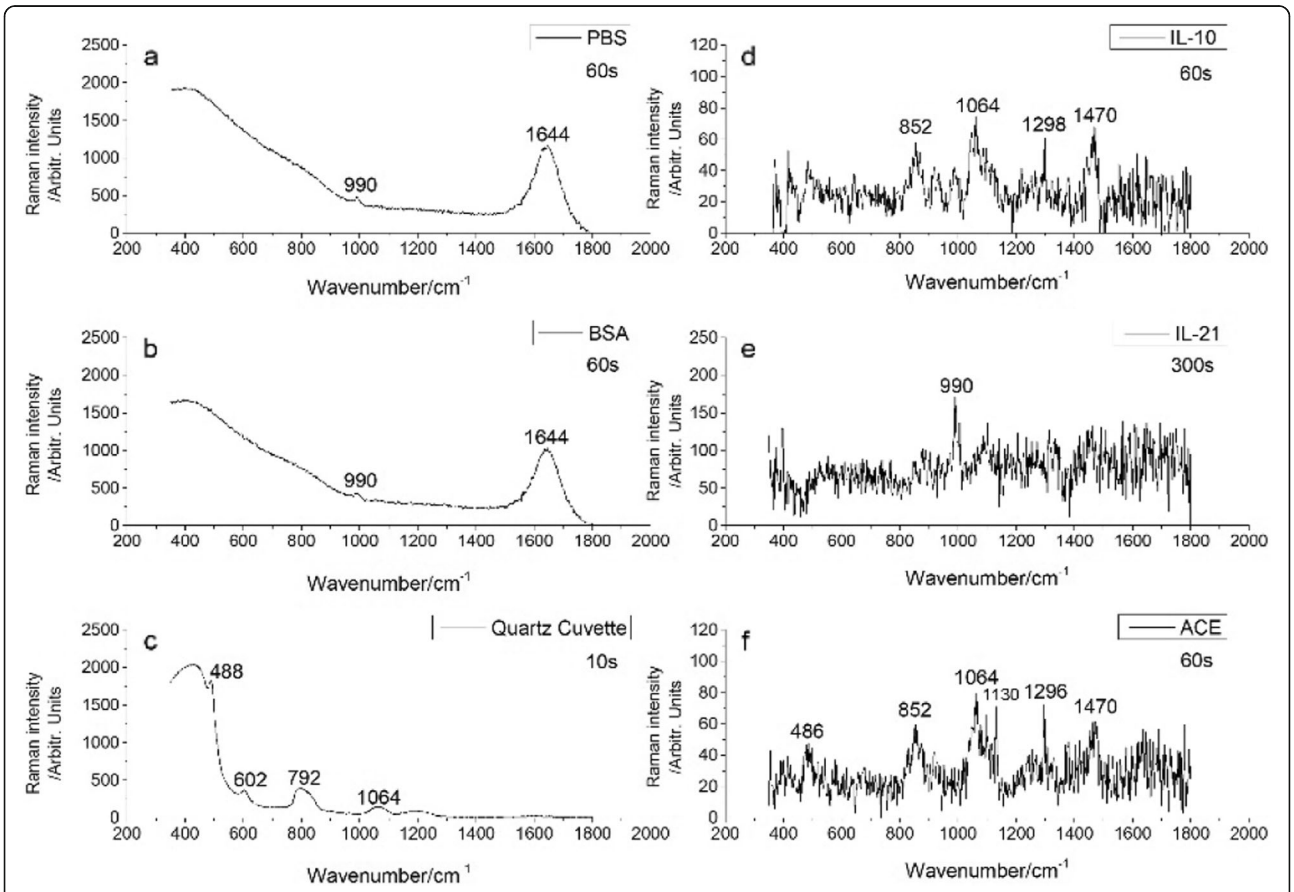

Fig. 1 Raman spectra obtained from background reference and samples. Spectrum from background refence of PBS(**a**), BSA(**b**), and fused silica cuvette, spectrum of samples from IL-10(**d**), IL-21(**e**), and ACE (**f**)

cm^{-1} in each spectrum, where there is no Raman signal but only spectral noise [22]. Raman spectra of PBS, 0.1% BSA and the fused silica cuvettes were obtained using the same experimental conditions for background correction and comparison.

Results

Figure 1 shows Raman spectra of PBS, BSA, fused silica cuvette, IL-10, IL-21 and ACE. In the wavenumber region between 350 cm^{-1} and 1800 cm^{-1}, Raman spectra of PBS (Fig. 1a) and BSA (Fig. 1b) both show a peak at 990 cm^{-1} and a water band at 1644 cm^{-1}. For the fused silica cuvette material (Fig. 1c), bands centered at 430 cm^{-1}, 488 cm^{-1}, 602 cm^{-1}, 792 cm^{-1} and 1064 cm^{-1} can be observed. The Raman band at 430 cm^{-1} is assigned to symmetric stretching mode of oxygen in a disordered 5- and 6- membered ring of SiO_4 tetrahedra. The peaks at 488 and 602 cm^{-1} are assigned to 4- and 6-membered rings of SiO_4 in the random network of the silica glass [23–25]. The bands centered at 1064 and 1200 cm^{-1} are attributed, respectively, to transverse-optical and longitudinal-optical components of the three-fold degenerate antisymmetric Si-O-Si stretch mode [24]. Similarly, the asymmetric band near 792 cm^{-1} is assigned to the threefold-degenerate "rigid cage" vibrational mode of SiO_2 units [24]. For IL-10 (Fig. 1d) we found peaks at 852, 1064, 1298 and 1470 cm^{-1}. The peak at 852 cm^{-1} might be from proline, hydroxyproline and tyrosine, 1298 cm^{-1} is suspected from CH_2 deformation modes and 1470 cm^{-1} can be assigned to a C=N stretching bond within the IL-10 protein structure [9]. For the spectra of IL-10, the SNR of highest peak at 1064 cm^{-1} is 5.02. Only a single peak at 990 cm^{-1} is found in IL-21 spectra (Fig. 1e) with SNR of 6.10. We did not find any identifiable Raman peaks within the high wavenumber region between 2500 and 4000 cm^{-1}, except for the broad water band between 3200 and 3500 cm^{-1} from the solvent. ACE (Fig. 1f) showed peaks at 486, 852, 1064, 1130,1296 and 1470 cm^{-1}. The peak at 852 cm^{-1} is from single bond stretching vibrations of the amino acids, valine, polysaccharides and tyrosine (Fermi resonance of ring fundamental and overtone) [26, 27]. The peak at 1130 cm^{-1} may be assigned to C-C skeletal stretch transconformation, whereas the peak at 1296 cm^{-1} comes from CH_2 deformation [28]. However, some peaks can also be seen in cuvette results, like the peaks at 600, 792 and 1064 cm^{-1}. The SNR of highest peak at 1064 cm^{-1} in ACE spectra is 6.15.

Discussion

To our knowledge, this is the first report of characteristic Raman spectra of IL-10 and ACE. For IL-10 we found characteristic Raman peaks at 852, 1296 and 1470 cm^{-1}. ACE is characterized by peaks located at 852, 1130, 1296 and 1470 cm^{-1}. The peak location at 486 cm^{-1} can be considered the same as fused silica cuvette peak at 488 cm^{-1}, since the spectral resolution of the spectrometer is 2 cm^{-1}. The peak observed at 990 cm^{-1} in IL-21 is most probably be attributed to a Raman signal from the additives of PBS [29]. We did not find additional peaks in the high wavelength region besides the water band.

For validating the characteristic peaks from the IL-10, IL-21 and ACE samples, background spectra from PBS and BSA were acquired. For error estimation between measurements, we calculated the coefficient of variation relative standard deviation (CVRSD) of each sample [30]. The CVRSD of BSA, PBS, IL-10, ACE and IL-21 are 0.89%, 0.73%, 1.68%, 1.68% and 1.25%, respectively. The peak at 990 cm^{-1} can be found both in PBS and BSA, which indicates no extra peaks will be picked up in the given concentration of our BSA samples. Hence, the 990 cm^{-1} peak found at IL-21 with 300 s integration time is most probably from PBS even the background already subtracted, due to the slight variance introduced by long integration times. Spectra from the fused silica cuvette were obtained by shifting the laser focus onto cuvette itself. Fused silica shows several Raman peaks, one of which, at 1064 cm^{-1}, that was observed in the spectra of IL-10 and ACE. Although the Raman signal intensity is relatively high with 10s integration time when focusing on the cuvette material, the use of the confocal system ensures only a minimal contribution from cuvette when focusing at the sample within the cuvette. We analyzed multiple spectra acquired from each sample. The repeatability of the results can be further improved by measuring more individual samples, which unfortunately were not available in the study.

Biological fluids are complex mixtures, which contain variants compounds [31], which may have multiple intra-molecular bonds in common. In our case, IL-10 and ACE share peaks at 852, 1296 and 1470 cm^{-1}. Only using one single peak to distinguish the proteins of interest from the diverse array of other proteins and other molecules present might lead to a biased conclusion. The 1130 cm^{-1} peaks only exist in ACE spectra and thus is helpful to differentiate ACE from IL-10. An even more complicated situation originates if each peak in the obtained spectra is an integrated result from all compounds it contains. In this case, more advanced data processing techniques are needed. Several techniques are proposed for pre- and post-processing Raman data, however, a well-accepted standard procedure is still lacking [32]. While testing biomolecules, the major challenge of Raman spectroscopy is its low detection limit. In addition, for low concentration samples, the SNR might below the limit of quantitation due to the fluorescence interference. A technique was proposed which requires a

wavelength tunable laser for sequentially shifting of excitation wavelength [11], however, having a fixed wavelength excitation laser, we were unable to use this approach. An alternative approach is to use peak intensity ratios of each compound to identify each compound independently and quantify its concentration. This peak intensity ratio approach already has been reported and validated for ex vivo Raman investigation in human aqueous humor [33]. In a previous study, we developed a tailored MATLAB (Version 2017b, The Mathworks Inc., Natick, MA, United States) data processing program for in vitro and in vivo Raman detection of ocular drug topically delivered to the animal eyes [34, 35] and demonstrated that with proper data processing, the molecular information can be extracted non-invasively from biological fluids in-situ and ex vivo.

Conclusions

Raman spectra of IL-10 and ACE were successfully obtained by our confocal Raman system. The SNR of Raman spectra could be further improved. The identification of IL-10 and ACE characteristic Raman peaks shows the potential possibilities for non-invasive investigation in the molecular level, which might help us better understanding the complex underlying the pathophysiology of diseases.

Abbreviations

IL-10: Interleukin-10; IL-21: Interleukin-21; ACE: Angiotensin Converting Enzyme; MS: Mass Spectrometry; BSA: Bovine Serum Albumin; PBS: Phosphate Buffered Saline; SNR: Signal-to-Noise Ratio; CVRSD: Coefficient Of Variation Relative Standard Deviation; SERS: Surface Enhanced Raman Spectroscopy; HPLC: High Performance Liquid Chromatography; PC: Pyro-Concentrator

Acknowledgements

We thank M. Tempelman from the Translational Immunology department of University Medical Center Utrecht for providing the IL-10, IL-21 and ACE samples.

Authors' contributions

All authors conceived of and designed the experimental protocol. SZ and FM performed the experiment and collected the data. All authors were involved in the analysis and interpretation of the data. SZ wrote the draft of the manuscript. FM, RE, CW, TB reviewed and revised the manuscript and produced the final version. All authors read and approved the final manuscript.

Funding

S. Zhang acknowledges the China Scholarship Council for the support by State Scholarship Fund No. 201309110103.

Availability of data and materials

Upon request to the authors.

Declarations

Competing interests

The authors declare that they have no competing interests.

Received: 11 August 2020 Accepted: 8 April 2021
Published online: 20 April 2021

References

1. Kuiper, J.J., et al.: An Ocular Protein Triad Can Classify Four Complex Retinal Diseases. Sci Rep. **7**, 41595 (2017)
2. Iyer, S.S., Cheng, G.: Role of interleukin 10 transcriptional regulation in inflammation and autoimmune disease. Crit. Rev. Immunol. **32**(1), 23–63 (2012). https://doi.org/10.1615/CritRevImmunol.v32.i1.30
3. Spolski, R., Leonard, W.J.: Interleukin-21: a double-edged sword with therapeutic potential. Nat. Rev. Drug Discov. **13**(5), 379–395 (2014). https://doi.org/10.1038/nrd4296
4. Bernstein, K.E., Khan, Z., Giani, J.F., Cao, D.Y., Bernstein, E.A., Shen, X.Z.: Angiotensin-converting enzyme in innate and adaptive immunity. Nat Rev Nephrol. **14**(5), 325–336 (2018). https://doi.org/10.1038/nrneph.2018.15
5. de Jager, W., Prakken, B.J., Bijlsma, J.W.J., Kuis, W., Rijkers, G.T.: Improved multiplex immunoassay performance in human plasma and synovial fluid following removal of interfering heterophilic antibodies. J. Immunol. Methods. **300**(1–2), 124–135 (2005). https://doi.org/10.1016/j.jim.2005.03.009
6. Smith, W.E.: Practical understanding and use of surface enhanced Raman scattering/surface enhanced resonance Raman scattering in chemical and biological analysis. Chem. Soc. Rev. **37**(5), 955–964 (2008). https://doi.org/10.1039/b708841h
7. Pannico, M., et al.: Direct printing of gold nanospheres from colloidal solutions by pyro-electrohydrodynamic jet allows hypersensitive SERS sensing. Appl Surface Sci. **531**, (2020)
8. Pelletier, C.C., Lambert, J.L., Borchert, M.: Determination of glucose in human aqueous humor using Raman spectroscopy and designed-solution calibration. Appl. Spectrosc. **59**(8), 1024–1031 (2005). https://doi.org/10.1366/0003702054615133
9. Movasaghi, Z., Rehman, S., Rehman, I.U.: Raman spectroscopy of biological tissues. Appl. Spectrosc. Rev. **42**(5), 493–541 (2007). https://doi.org/10.1080/05704920701551530
10. Li, Z., et al.: A Plasmonic Staircase Nano-Antenna Device with Strong Electric Field Enhancement for Surface Enhanced Raman Scattering (SERS) Applications. J Phys D: Applied Physics. **45**, 30 (2012)
11. Marshall, S., Cooper, J.B.: Quantitative Raman spectroscopy when the signal-to-noise is below the limit of quantitation due to fluorescence interference: advantages of a moving window sequentially shifted excitation approach. Appl. Spectrosc. **70**(9), 1489–1501 (2016). https://doi.org/10.1177/0003702816662621
12. Grilli, S., et al.: Active Accumulation of Very Diluted Biomolecules by Nano-Dispensing for Easy Detection below the Femtomolar Range. Nature Commun. **5**, 5314 (2014)
13. Rega, R., et al.: Detecting Collagen Molecules at Picogram Level through Electric Field-Induced Accumulation. Sensors (Basel). **20**, 12 (2020)
14. Kupcova Skalnikova, H., et al.: Advances in Proteomic Techniques for Cytokine Analysis: Focus on Melanoma Research. Int J Mol Sci. **18**, 12 (2017)
15. Xu, K., et al.: Micro Optical Sensors Based on Avalanching Silicon Light-Emitting Devices Monolithically Integrated on Chips. Optical Materials Express. **9**, 10 (2019)
16. Xu, K., et al.: Light Emission from a Poly-Silicon Device with Carrier Injection Engineering. Materials Sci Engineering: B. **231**, 28–31 (2018)
17. Erckens, R., et al.: Raman spectroscopy in ophthalmology: from experimental tool to applications in vivo. Lasers Med. Sci. **16**(4), 236–252 (2001). https://doi.org/10.1007/PL00011360
18. Erckens, R.J., Jongsma, F.H.M., Wicksted, J.P., Hendrikse, F., March, W.F., Motamedi, M.: Drug-induced corneal hydration changes monitoredin vivo by non-invasive confocal Raman spectroscopy. J. Raman Spectrosc. **32**(9), 733–737 (2001). https://doi.org/10.1002/jrs.731
19. Elshout, M., Erckens, R.J., Webers, C.A., Beckers, H.J., Berendschot, T.T., de Brabander, J., Hendrikse, F., Schouten, J.S.: Detection of Raman spectra in ocular drugs for potential in vivo application of Raman spectroscopy. J. Ocul. Pharmacol. Ther. **27**(5), 445–451 (2011). https://doi.org/10.1089/jop.2011.0018
20. Kaji, Y., et al.: Raman Microscopy: a Noninvasive Method to Visualize the Localizations of Biomolecules in the Cornea. Cornea. **36**(Suppl 1), S67–S71 (2017)
21. Paluszkiewicz, C., Chaniecki, P., Rękas, M., Rajchel, B., Piergies, N., Kwiatek, W. M.: Analysis of human lenses by Raman microspectroscopy. Acta Phys. Pol. A. **129**(2), 244–246 (2016). https://doi.org/10.12693/APhysPolA.129.244

22. Lazaro, J.C., et al.: Optimizing the Raman signal for characterizing organic samples: the effect of slit aperture and exposure time. Spectrosc-Int J. **23**(2), 71–80 (2009). https://doi.org/10.1155/2009/764524
23. Awazu, K., Kawazoe, H.: Strained Si–O–Si bonds in amorphous SiO2 materials: a family member of active centers in radio, photo, and chemical responses. J. Appl. Phys. **94**(10), 6243–6262 (2003). https://doi.org/10.1063/1.1618351
24. Galeener, F.L.: Band limits and the vibrational spectra of tetrahedral glasses. Phys. Rev. B. **19**(8), 4292–4297 (1979). https://doi.org/10.1103/PhysRevB.19.4292
25. Galeener, F.L.: Planar rings in vitreous silica. J. Non-Cryst. Solids. **49**(1), 53–62 (1982). https://doi.org/10.1016/0022-3093(82)90108-9
26. Gniadecka, M., Wulf, H.C., Nymark Mortensen, N., Faurskov Nielsen, O., Christensen, D.H.: Diagnosis of basal cell carcinoma by Raman spectroscopy. J. Raman Spectrosc. **28**(23), 125–129 (1997). https://doi.org/10.1002/(SICI)1097-4555(199702)28:2/3<125::AID-JRS65>3.0.CO;2-#
27. Shetty, G., Kendall, C., Shepherd, N., Stone, N., Barr, H.: Raman spectroscopy: elucidation of biochemical changes in carcinogenesis of oesophagus. Br. J. Cancer. **94**(10), 1460–1464 (2006). https://doi.org/10.1038/sj.bjc.6603102
28. Faolain, E.O., et al.: A study examining the effects of tissue processing on human tissue sections using vibrational spectroscopy. Vib. Spectrosc. **38**(1), 121–127 (2005). https://doi.org/10.1016/j.vibspec.2005.02.013
29. C. David et al., "Raman and IR Spectroscopy of Manganese Superoxide Dismutase, a Pathology Biomarker," *Vibrational Spectroscopy* 62(50–58 (2012)
30. F. J. H. Douglas A. Skoog, Stanley R. Crouch, *Principles of Instrumental Analysis*, 7th ed., Cengage Learning (2016)
31. L. M. Levine, "Basic and Clinical Science Course, Section 2: Fundamentals and Principles of Ophthalmology," in *Basic and Clinical Science Course*, p. 430, American Academy of Ophthalmology (2018–2019)
32. Byrne, H.J., Knief, P., Keating, M.E., Bonnier, F.: Spectral pre and post processing for infrared and Raman spectroscopy of biological tissues and cells. Chem. Soc. Rev. **45**(7), 1865–1878 (2016). https://doi.org/10.1039/C5CS00440C
33. Woong Moon, S., Kim, W., Choi, S., Shin, J.H.: Label-free optical detection of age-related and diabetic oxidative damage in human aqueous humors. Microsc. Res. Tech. **79**(11), 1050–1055 (2016). https://doi.org/10.1002/jemt.22743
34. C. J. F. Bertens et al., "Confocal Raman spectroscopy: Evaluation of a non-invasive technique for the detection of topically applied ketorolac tromethamine in vitro and in vivo," *Int. J. Pharm.* 570(118641 (2019)
35. S. Zhang et al., "in Vitro and in Vivo Datasets of Topically Applied Ketorolac Tromethamine in Aqueous Humor Using Raman Spectroscopy," *Data Brief* 27(104694 (2019)

Publisher's Note